Unusually Strong Optical Interactions between Particles in Quasi-One-Dimensional Geometries

Raquel Gómez-Medina and Juan José Sáenz

Departamento de Física de la Materia Condensada and Instituto "Nicolás Cabrera," Universidad Autónoma de Madrid, E-28049 Madrid, Spain

(Received 24 March 2004; published 9 December 2004)

A theoretical analysis of the optically induced interaction between small particles in a quasi-one-dimensional system is presented. The total reflection of light modes near a geometric resonance leads to strong radiation pressure on a single particle. The presence of the two particles splits the resonance leading to a nontrivial oscillating interaction. The existence of stable, optically bound dimers under two counterpropagating (noncorrelated) light modes is also discussed.

DOI: 10.1103/PhysRevLett.93.243602 PACS numbers: 42.50.Vk, 32.80.Lg, 42.25.Bs

By fashioning proper optical field gradients it is possible to trap and manipulate small particles with *optical tweezers* [1,2] or create atomic arrays in optical lattices [3]. Intense optical fields can also induce significant forces *between* particles [4,5]. In analogy with atomic physics, the resonant modes of a single particle play the role of electronic orbitals [6] and, like their electronic counterparts, could lead to bonding and antibonding interactions between neighboring particles [7]. Far from the particle resonances, light forces are, in general, very small. However, when the fields are confined in quasi-one-dimensional (Q1D) waveguide structures, the coupling of the scattered dipolar field with the waveguide modes leads to a resonant state close to the threshold of a new propagating mode [8]. Just at the resonance, the effective cross section of a single particle becomes of the order of the wavelength leading to a enhanced resonant radiation pressure [8,9]. The main purpose of this work is to show that these *geometric* resonances lead to unusual strong optical interactions *between* particles.

Geometric resonances had been discussed in the context of electronic transport through a Q1D wire. In the presence of a single pointlike attractive impurity, the electronic conductance was shown to present pronounced asymmetric dips close to the onset of a new propagating channel [10–13]. Similar geometric resonances appear in the context of ultracold atomic collisions in confined geometries [14]: as in the electronic case, the scattering process between two atoms confined in a Q1D system can degenerate to a total reflection [14]. As we will see, the light scattering by two small particles leads to a nontrivial splitting of the geometric resonance. Interestingly, the splitting of the resonance does not always correspond to the expected familiar bonding-antibonding picture of atomic physics. We will also show that, under the presence of two counterpropagating (noncorrelated) wave modes, the interaction potential can be tuned to present a deep minimum leading to a stable optically bound dimer.

For the sake of simplicity we consider a two-dimensional xz waveguide. The pointlike particles are then represented by two similar cylinders located at $\vec{r}_1 = (x_1, z_1)$ and $\vec{r}_2 = (x_2, z_2)$ (lying along the oy axis) with radius much smaller than the wavelength. An s-polarized electromagnetic wave is assumed (the electric field parallel to the cylinder axis), $\vec{E}^{\text{in}}(\vec{r}) = \exp(-i\omega t)E^{\text{in}}(\vec{r})\vec{u}_y$. The transversal confinement define a set of guided modes with wave numbers $k_n^2 = (\omega^2 - \omega_n^2)/c^2$ $(\omega_1 < \omega_2 < \dots)$ and transversal eigenfunctions $\phi_n(x)$. For a single mode waveguide $(\omega_1 < \omega < \omega_2)$ an incoming electric field can be written as

$$E^{\text{in}}(\vec{r}) = E_0\left\{\frac{1}{\sqrt{k_1}}\phi_1(x)\exp[ik_1 z]\right\}. \tag{1}$$

Each scatterer is characterized by its *scattering amplitude* in the unbounded free-space $4\pi f$ [15]. The total field E in the waveguide is given by the incoming field plus the fields scattered from each particle, $E = E^{\text{in}} + \sum_i E_i^{\text{sc}}$, with

$$E_i^{\text{sc}}(\vec{r}) = 4\pi f E_{\text{inc}}(\vec{r}_i)[G_0(\vec{r}, \vec{r}_i) + G_b(\vec{r}, \vec{r}_i)], \tag{2}$$

where $E_{\text{inc}}(\vec{r}_i)$ is the incident field on the i particle and $G = G_0 + G_b$ is the waveguide Green function. G_0 is the outgoing unbounded free-space Green function corresponding to waves *emerging* from the particle and G_b, the regular part of the Green function, corresponds to the waves scattered from the walls [16]. The time averaged dipolar force on the i particle is given by [17]:

$$\vec{F}_i = \frac{\epsilon_0 c^2}{2\omega^2}\Re\{4\pi f E_{\text{inc}}(\vec{r}_i)\nabla E_{\text{inc}}^*(\vec{r})\}_{\vec{r}=\vec{r}_i}. \tag{3}$$

For a single scatterer, the actual field *incident* on the particle is given by

$$E_{\text{inc}}(\vec{r}) = E^{\text{in}}(\vec{r}) + E_{\text{inc}}(\vec{r}_1)4\pi f G_b(\vec{r}, \vec{r}_1). \tag{4}$$

The multiple scattering processes between the scatterer and the lateral confinement lead to a *renormalized scattering amplitude* [11]

$$4\pi\hat{f} = \left(\Re\left\{\frac{1}{4\pi f} - G_b\right\} - i\Im\{G\}\right)^{-1}, \tag{5}$$

with $G_b = \lim_{\vec{r}\to\vec{r}_1}[G(\vec{r}, \vec{r}_1) - G_0(\vec{r}, \vec{r}_1)]$ [16] and, for a

single mode waveguide, $\Im\{G\} = \phi_1^2(x_1)/(2k_1)$. The transmission amplitude t and the transmission probability $T = |t|^2$ are simply related to $4\pi\hat{f}$ through

$$t = 1 + i4\pi\hat{f}\Im\{G\}. \tag{6}$$

From Eqs. (3)–(6) we find that the forward force on the particle is simply given by

$$F_z = F_{\max}(1 - T) \quad \text{with} \quad F_{\max} = \frac{\epsilon_0 c^2 |E_0|^2 k_1}{\omega^2}. \tag{7}$$

Transversal forces are mainly given by polarization forces (i.e., proportional to the field intensity gradient) [8]:

$$F_x \approx -\frac{\partial}{\partial x_1} U(x_1) = \frac{F_{\max}}{2k_1} \frac{\partial}{\partial x_1} [\Re\{4\pi\hat{f}\}\Im\{G\}]. \tag{8}$$

For weak "attractive" scatterers $\Re\{1/(4\pi f)\} > 0$ is large and dominates the renormalized scattering amplitude. The forward radiation pressure is then very small and the confining potential U slightly attracts the particle towards the center of the guide (where $\Im\{G\}$ is maximum). However, approaching the cutoff frequency ω_2 (i.e., below the threshold of a new propagating mode), $k_2 = i\kappa_2$ goes to zero. Then, the contribution of the evanescent mode to $\Re\{G_b\}$ outweighs all the others and $\Re\{G_b\} \approx \phi_2^2(x_1)/(2\kappa_2)$ diverging at the threshold [16]. The precise compensation of these two large terms at $\omega \approx \omega_0$ gives rise to a geometric resonance. The geometric resonance can be seen as a Feshbach resonance [18]: It occurs when the energy (frequency) of the incoming wave is tuned to the energy (frequency) of the geometry-induced quasi bound state (QBS) [19]. Based on general arguments [12], the Q1D transmission resonances are then expected to exhibit the asymmetric Fano line shape characteristic of Feshbach-type resonances [18] $T(\varepsilon) \propto (q + \varepsilon)^2/(\varepsilon^2 + 1)$. For classical waves, $\varepsilon = (\omega - \omega_r)/\Gamma$ (ω_r and Γ being the frequency and frequency width of the resonance). As a matter of fact, expanding Eq. (6), we find

$$T(\omega) \approx \frac{(\omega - \omega_0)^2}{(\omega - \omega_0)^2 + 2q\Gamma(\omega_2 - \omega)}, \tag{9}$$

with $\kappa_2 = |k_2|$, $q = \Im\{G\}/\Re\{1/(4\pi f)\} \ll 1$, and $\Gamma = 2(\omega_2 - \omega_0)q$, which has the expected Fano shape with $\omega_r = \omega_0 + q\Gamma$ [20]. The forward force obtained through this approximated expression can be compared (see Fig. 1) with the exact results for the force on a small dielectric cylinder inside a waveguide with perfectly conducting walls and cross length D [8,16].

Let us turn back to the problem with two similar particles. The self-consistent *incident* field around each particle is now given by the sum of three terms: the incoming field E^{in} and the backscattered fields from the walls and from the other particle:

$$E^i_{\text{inc}}(\vec{r}) = E^{\text{in}}(\vec{r}) + 4\pi f E_{\text{inc}}(\vec{r}_i) G_b(\vec{r}, \vec{r}_i) + 4\pi f E_{\text{inc}}(\vec{r}_j) G(\vec{r}, \vec{r}_j). \tag{10}$$

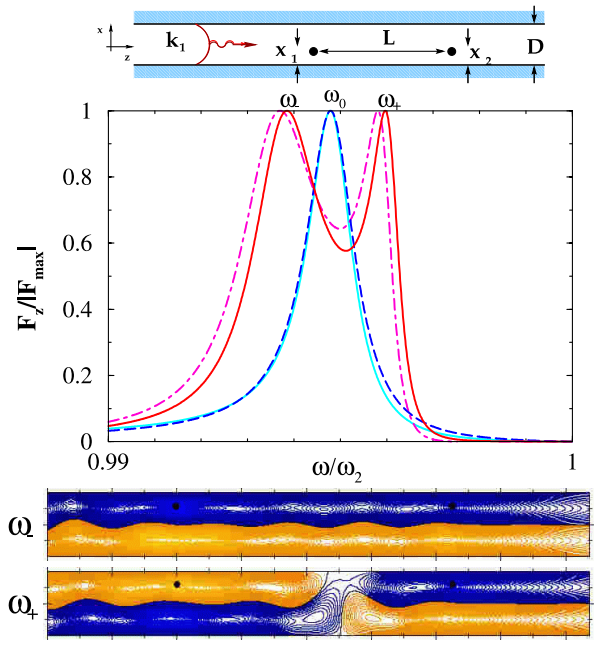

FIG. 1 (color online). Normalized total forward force $[F_z/|F_{z_{\max}}| = (1 - T)]$ vs ω on a single particle (single peak) and on the two particle system (double peak) at $k_1 L/\pi = 7.4$. Dashed and dot-dashed curves corresponds to the approximated expressions (9) and (13) (with no fitting parameters). (Top: sketch of the particle-waveguide system. Bottom: Patterns of the real part of the total electric field at the resonant frequencies (ω_-, ω_+).

Once we know the incident fields, the forces acting on each particle follow directly from Eq. (3). For frequencies close to the single-particle resonance $\omega \approx \omega_0$ we found that the lateral confining potential is dominated by the renormalized scattering amplitude (proportional to $\phi_2^2(x_1)$ [8]) being approximately independent on the relative position of the particles. For simplicity we will then assume that the particles are confined around the potential minimum (for a hard-wall waveguide, $x_1 = x_2 \approx D/4$). For each particle, the renormalized amplitude is given by

$$4\pi\hat{\hat{f}}_i = \frac{1 + 4\pi\hat{f} G_{ij} e^{ik_1(z_j - z_i)}}{1 - (4\pi\hat{f} G_{ij})^2} 4\pi\hat{f}, \tag{11}$$

with $G_{ij} = G_{ji} = G(\vec{r}_i, \vec{r}_j)$ and the transmission amplitude reads as

$$t = 1 + i\{4\pi\hat{\hat{f}}_1 + 4\pi\hat{\hat{f}}_2\}\Im\{G\}. \tag{12}$$

We can now calculate the forward forces acting on each particle F_{z1} and F_{z2}, the total forward force $[F_z = F_{\max}(1 - |t|^2) = F_{z1} + F_{z2}]$ and the effective interaction force *between* particles $F_{12} = F_{z2} - F_{z1}$. In Fig. 1 we plot F_z (solid line) versus frequency for the same parameters as the single-particle system at a fixed distance L between particles ($k_1 L/\pi = 7.4$). As we might expect, the overlap of the scattered fields leads to a splitting of the geometric

resonance. However, the analysis of the splitting as a function of the particle distance reveals an unexpected complex behavior.

In Fig. 2(a) we show a contour plot of the total force [$\propto(1-T)$] in a frequency distance ($\omega - k_1 L$) map (the F_z vs ω curve in Fig. 1 corresponds to the vertical line at $k_1 L/\pi = 7.4$). The force/transmission resonances manifest themselves as oscillating scars above and below the single-particle resonance frequency. Interestingly, depending on $k_1 L$ we can find two resonant frequencies, one resonance or even no resonance at all. In order to understand this complex behavior, we have analyzed the splitting phenomena very close to the Fano-Feschbach resonance. Expanding the renormalized scattering amplitudes near $\omega \approx \omega_0$ we find that the transmittance T can be written as

$$T \simeq \frac{((\omega_p - \omega)^2 - \delta^2)2}{[((\omega_p - \omega)^2 - \delta^2) - \chi(\omega_2 - \omega)]^2 + 2q\hat{\Gamma}(\omega_c - \omega)^2(\omega_2 - \omega)}, \tag{13}$$

where

$$\omega_p \approx \omega_0 + \delta_L q \sin(k_1 L), \qquad \delta_L = 2(\omega_2 - \omega_0)e^{-\kappa_2 L}, \qquad \delta \approx \sqrt{\delta_L[\delta_L - 2\Gamma \sin(k_1 L)]}, \qquad \chi = 4q\Gamma \sin^2(k_1 L),$$
$$\eta = [1 - q \sin(2k_1 L)/2], \qquad \hat{\Gamma} = 4\Gamma\eta^2, \qquad \omega_c \approx \omega_0 + \eta^{-1}\cos(k_1 L)[\delta_L - \Gamma \sin(k_1 L)].$$

Equation (13) provides a qualitative explanation of all the observed features in the force map [Fig. 2(a)]: For fixed L, the total force (the transmittance) seems to present two maxima (two zeros) at $\omega_\pm = \omega_p \pm \delta$. At short distances the splitting ($\propto \delta_L$) is roughly given by the overlap between the evanescent scattered fields which play the same role as the exponentially decaying orbitals in atomic systems. However, for $k_1 L \approx n\pi$ [i.e., $\sin(k_1 L) = 0$, $\cos(k_1 L) = \pm 1$], interference destroy one of the two maxima and the total force presents a single maximum at $\omega \approx \omega_0 - (-1)^n \delta_L$. At larger distances, both resonances disappear whenever $\exp(-\kappa_2 L) < 2q \sin(k_1 L)$. For these relatively large distances the splitting is small and, as shown in Fig. 1, there is a remarkable quantitative agreement between the approximated result (with no fitting parameters) and the exact calculation. In general, for $\omega \approx \omega_-$ the electric fields around the particles shows a symmetric pattern while for $\omega \approx \omega_+$ it is antisymmetric (bottom of Fig. 1).

The actual nature of the resonances is obtained from Fig. 2(b) where we plot the effective interaction force map, F_{12} vs L. The contour lines define the limit between "bonding" ($F_{12} < 0$) and "antibonding" ($F_{12} > 0$) regions. In the bonding regions, the total forward force is focused on particle one leading to an effective "attrac-

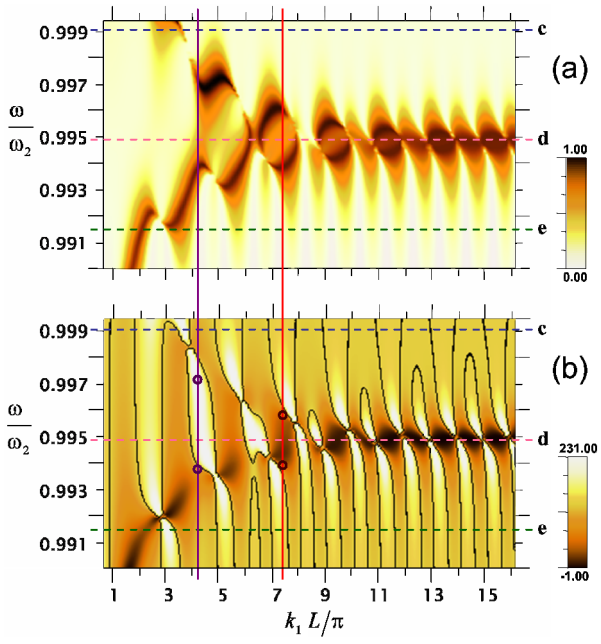

FIG. 2 (color online). (a) Contour plot of the normalized total forward force ($F_z = F_{z2} + F_{z1}$) and (b) normalized interaction force *between* particles ($F_{12} = F_{z2} - F_{z1}$) in a frequency-distance ($\omega - k_1 L$) map. Contour lines in (b) correspond to $F_{12} = 0$ separating bonding and antibonding regions. Vertical lines at $k_1 L/\pi = 7.4$ and $k_1 L/\pi = 4.3$ correspond to the F_z vs ω curves in Figs. 1 and 3, respectively [circles on the lines in (b) are at the resonant peaks in (a)].

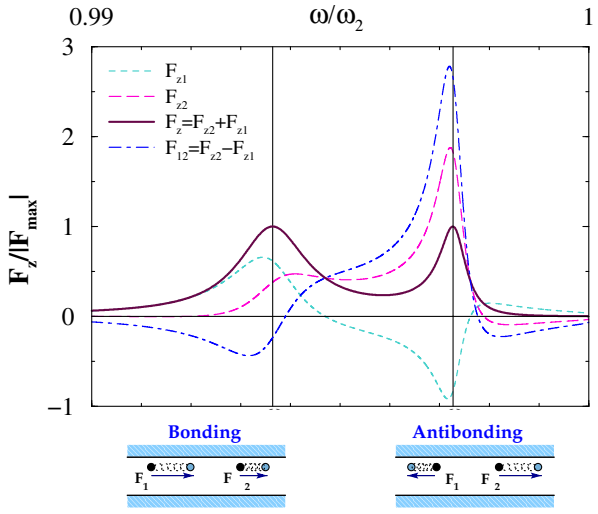

FIG. 3 (color online). Normalized forces vs frequency for the two particles system at $k_1 L/\pi = 4.3$. The continuous line represents the total forward force F_z. Dotted and dashed lines correspond to F_{z1} and F_{z2}, respectively. Dot-dashed curve represents the interaction force between particles F_{12}.

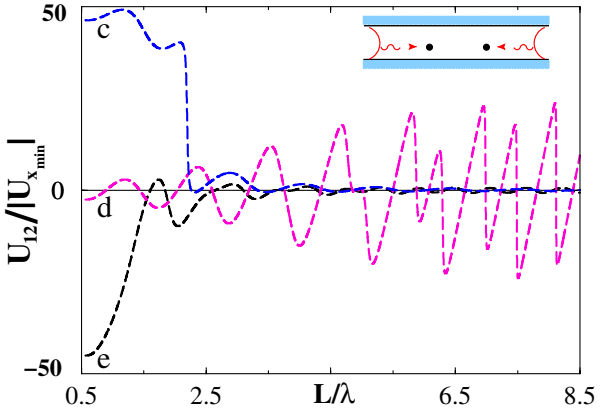

FIG. 4 (color online). Optically induced interaction potential between two particles at a distance L for three different frequencies (corresponding to the horizontal lines of Fig. 2).

tion" between particles. In the antibonding regions the effective repulsion comes from the radiation pressure of the scattered wave *between* the two particles: there is a forward force on particle 2 ($F_{z2} > 0$) whereas particle 1 is pushed backwards ($F_{z1} < 0$). This is illustrated in Fig. 3 where we have plotted the different forces F_{zi}, F_{12}, and F_z vs ω for $k_1 L/\pi = 4.3$. When the splitting is dominated by the evanescent scattered fields, the nature of the resonant peaks corresponds to the familiar bonding-antibonding picture. However, for larger distances, the interaction at the resonant frequencies is always attractive (for example, both peaks in Fig. 1 correspond to bonding interactions).

The forward forces can be compensated if the waveguide is excited by two equivalent counterpropagating modes. If these two modes are uncorrelated (i.e., mutually incoherent), the total time average force is simply the sum of the forces induced by each wave mode. In this case, there is no net force on the two particle system ($F_z = 0$) and we can derive a *light-induced interaction potential* between the particles, $2(F_{z2} - F_{z1}) \approx -(\partial/\partial L)U_{12}(L)$. In Fig. 4 we plot the interaction potential as a function of the distance L for three different frequencies (corresponding to the three horizontal lines in Fig. 2). In general, $U(L)$ presents a background oscillating behavior. For frequencies larger than ω_0 there is an average antibonding interaction while for lower frequencies the particles attract each other. The effective interaction potential can then be tuned to present a deep minimum leading to a stable optically bound dimer.

In summary, we have analyzed the optical interactions between small particles in a quasi-one-dimensional system near a geometric resonance. In contrast with the forces associated to internal Mie modes, optically induced interactions in Q1D could be tuned and manipulated by appropriated control of the confining geometry.

This work has been supported by the Spanish MCyT (Ref. No. BFM2003-01167) and the "Molecular Imaging" EU-IP project (LSHG-CT-2003-503259).

[1] A. Ashkin, Phys. Rev. Lett. **24**, 156 (1970); Science **210**, 1081 (1980); Proc. Natl. Acad. Sci. U.S.A. **94**, 4853 (1997); A. Ashkin, J. M. Dziedzic, J. E. Bjorkholm, and S. Chu, Opt. Lett. **11**, 288 (1986).
[2] D. G. Grier, Nature (London) **424**, 810 (2003).
[3] P. Verkerk *et al.*, Phys. Rev. Lett. **68**, 3861 (1992); P. S. Jessen *et al.*, *ibid.* **69**, 49 (1992).
[4] M. M. Burns, J.-M. Fournier, and J. A. Golovchenko, Phys. Rev. Lett. **63**, 1233 (1989); Science **249**, 749 (1990).
[5] S A. Tatarkova, A. E. Carruthers, and K. Dholakia, Phys. Rev. Lett. **89**, 283901 (2002).
[6] M. Bayer *et al.*, Phys. Rev. Lett. **81**, 2582 (1998).
[7] M. I. Antonoyiannakis and J. B. Pendry, Phys. Rev. B **60**, 2363 (1999).
[8] R. Gómez-Medina *et al.*, Phys. Rev. Lett. **86**, 4275 (2001).
[9] For a single atom, geometric resonances can also induce huge Stark shifts in the atomic levels [P. Horak, P. Domokos, and H. Ritsch, Europhys. Lett. **61**, 459 (2003)].
[10] C. S. Chu and R. S. Sorbello, Phys. Rev. B **40**, 5941 (1989); P. F. Bagwell,*ibid.* **41**, 10 354 (1990); E. Tekman and S. Ciraci, *ibid.* **43**, 7145 (1991).
[11] Ch. Kunze, and R. Lenk, Solid State Commun. **84**, 457 (1992).
[12] E. Tekman and P. F. Bagwell, Phys. Rev. B **48**, 2553 (1993); J. U. Nöckel and A. D. Stone,*ibid.* **50**, 17 415 (1994).
[13] J. Göres *et al.*, Phys. Rev. B **62**, 2188 (2000).
[14] M. Olshanii, Phys. Rev. Lett. **81**, 938 (1998); T. Bergeman, M. G. Moore, and M. Olshanii, *ibid.* **91**, 163201 (2003); R. Stock, I. H. Deutsch, and E. L. Bolda, *ibid.* **91**, 183201 (2003).
[15] $4\pi f$ is related to the (real) polarizability $\alpha \equiv \epsilon_0 \Re\{4\pi f\}/k^2$ and the scattering cross section (cross length in 2D) $\sigma \equiv \Im\{4\pi f\}/k$.
[16] $G(\vec{r}, \vec{r}_i) = \sum_n \phi_n(x)\phi_n(x_i)[i \exp(ik_n|z - z_i|)/(2k_n)]$. For a waveguide with perfectly conducting walls and cross length D [following P. M. Morse and H. Feshbach, *Methods of Theoretical Physics* (McGraw-Hill, N.Y., 1953), Chap. 7] we obtain an exact analytical expression for G_b:

$$G_b(\vec{r}_i, \vec{r}_i) = \frac{1}{2}\sum_{n=1}^{\infty} \phi_n^2 \left\{\frac{i}{k_n} - \frac{D}{n\pi}\right\} + \frac{1}{2\pi}\ln\left(\frac{\alpha}{\pi}\phi_0\right) + C,$$

where $\alpha = (\omega D/c)\sqrt{(D/2)}$, $C = \gamma_E/(2\pi) - i/4$, and γ_E is the Euler constant.
[17] J. P. Gordon, Phys. Rev. A **8**, 14 (1973).
[18] H. Feshbach, Ann. Phys. (N.Y.) **5**, 357 (1958); **19**, 287 (1962); U. Fano, Phys. Rev. **124**, 1866 (1961).
[19] In the absence of propagating modes ($\omega < \omega_1$) $\Im\{G\} = 0$ and the resonant condition leads to $4\pi\hat{f} \to \infty$, characteristic of a real *bound state*. Above the lowest cutoff, the coupling with propagating modes transforms the bound state to a *quasi bound state* [11].
[20] Similar Fano line shapes for classical sound waves but associated to *internal* particle resonances have been recently observed [see C. Goffaux *et al.*, Phys. Rev. Lett. **88**, 225502 (2002)].